

1 Spatially Correlated Stand Structures:
2 A Simulation Approach using Copulas

3
4 John A Kershaw, Jr.^{1,*}

5 Evelyn W. Richards¹

6 James B. McCarter²

7 Sven Oborn¹

8
9
10 ¹Faculty of Forestry and Environmental Management, University of New Brunswick, PO Box
11 4400, Fredericton, NB E3B 5A3, Canada

12 ²Research Scientist, School of Forest Resources, College of the Environment, University of
13 Washington and Adjunct Associate Professor, Department of Forestry and Environmental
14 Resources, College of Natural Resources, North Carolina State University

15 *corresponding author

16

40 woodlands (Pommerening 2006). Several process based models and hybrid models have
41 emerged, and many of these models require spatial data including maps of individual tree
42 locations (e.g., Pretzsch 1992, Pacala et al. 1993, Courbaud 1995).

43 Initialization and testing projections of such models require adequate descriptions of
44 spatial distribution of trees in stands (Pukkala 1988). Collection of such data is generally time
45 consuming and expensive; therefore, very few datasets exists. As a result, several mechanisms
46 for generating spatial data have been proposed (e.g., Stoyan and Penttinen 2000, Valentine et al.
47 2000, Kokkila et al. 2002). Many growth models that require spatial data are highly sensitive to
48 initial stand structure (Valentine et al. 2000, Goreaud et al. 2004, 2006); therefore, it is
49 necessary to have stand structure generators capable of simulating realistic patterns of species
50 composition and spatial and size distribution patterns (Pretzsch 1997).

51 **2 EXISTING APPROACHES**

52 Most approaches, such as those of Valentine et al. (2000) and Kokkila et al. (2002), start
53 with a two-dimensional Poisson point process. Tree locations are generated using one of several
54 point process algorithms (e.g., Penridge 1986, Baddeley and Turner 2008). Depending on the
55 algorithm and parameter values, point patterns can vary from regular lattice processes
56 representing a single species, even-aged plantation to a highly clustered pattern as might be
57 found in a mixed species, uneven-aged stand. Some algorithms have the capability of
58 incorporating spatial inhomogeneity (Baddeley and Turner 2008).

59 Once tree locations (points in the point process) are determined, tree size and species
60 attributes are assigned. In some systems, this is done independently of the point pattern (e.g., Ek
61 and Monserud 1974). This approach ignores competitive interactions between individual trees
62 that greatly influence observed stand structure patterns (Valentine et al. 2000, Kokkila et al.

63 2002, Goreaud et al. 2004). Stand structures generated using such processes are often unrealistic
64 (Valentine et al. 2000, Kokkila et al. 2002), and can influence long-term growth projections
65 (Goreaud et al. 2006).

66 To avoid this problem, Valentine et al. (2000) utilized a multistep process to generate
67 initial stand structures used in the AMORPHYS model. In the first step, tree locations are
68 generated. Diameters are then sampled from a target distribution and assigned randomly to the
69 tree locations. The height of each model tree is then calculated from its assigned diameter and
70 distances to its neighbors. Next, crown length of each tree is calculated from its height and
71 distances to its neighbors. Finally, diameter is recalculated based on height and crown length.
72 While this resulting process produces realistic stand structures, the resulting diameter distribution
73 may deviate from the target distribution as a result of the recalculation step and require re-
74 simulation (Valentine et al. 2000).

75 An alternative approach is to use a marked point process model (Penttinen et al. 1992,
76 Mateu et al. 1998). In a marked point process model, points are tree locations in a Cartesian
77 coordinate system, and marks are qualitative characteristics such as tree species, or quantitative
78 characteristics such as stem diameter or height (Penttinen et al. 1992). Two correlation functions
79 characterize marked point processes (Penttinen et al. 1992): a pair correlation function which
80 characterizes variability within the system of tree locations; and a mark correlation function
81 which characterizes relationships between different sets of trees (marks) conditional on a
82 distance function.

83 Penttinen et al. (1992) provide excellent examples of the application of marked point
84 processes applied to modeling stand structure. Pommerening et al. (2000) and Mateu et al.
85 (1998) demonstrate the use of marked Gibbs processes to model forest stand structures and

86 discuss how these might be used to simulate forest stand structure. Kokkila et al. (2002)
87 developed a stand structure simulator building upon Penttinen et al.'s (1992), Pommerening et al.
88 (2000), Mateu et al.'s (1998), and others' work. Kokkila et al. (2002) combine marked Gibbs
89 processes with Markov chain Monte Carlo simulation to produce a flexible stand structure
90 simulator. In addition to the pair and mark correlation functions, they incorporate an additional
91 site potential function which provides additional control on the spatial distribution of trees within
92 simulated stands.

93 While these methods are able to generate structures that statistically resemble example
94 data, no general methods for estimating the parameters required to initialize the simulators are
95 presented (however, see Mateu et al. 1998 and Pommerening et al. 2000). In this paper we
96 present a new approach based on the methods of copulas (Genest and MacKay 1986) and
97 develop a simulation system in R (R Development Core Team 2009).

98 **3 MODELLING APPROACH**

99 Standard Normal copulas are utilized to transform random normal variables into
100 correlated variables. Copulas, though widely utilized in several other fields (Accioly and
101 Chiyoshi 2004, Yan 2007), are not very widely known, or at least not widely utilized, in forestry
102 and natural resource management.

103 A copula is a multivariate distribution whose marginals are all uniform over (0, 1). For a
104 p-dimensional random vector U on the unit cube, a copula C is:

$$105 \quad C(\mathbf{u}_1, \dots, \mathbf{u}_p) = \Pr(U_1 \leq \mathbf{u}_1, \dots, U_p \leq \mathbf{u}_p).$$

106 Because any continuous random variable can be transformed to be uniform over (0, 1) by its
107 probability integral transformation, copulas can be used to provide multivariate dependence
108 independent of marginal distributions (Genest and MacKay 1986, Nelsen 2006, Yan 2007). For

109 a complete treatment of the theory and basis of copulas see Nelsen (2006) and for a more
 110 descriptive treatment see Genest and MacKay(1986).

111 The basis of our approach assumes there is a correlation between a tree's characteristics
 112 (dbh, total height, and crown ratio) and the area available to the tree (Mitchell 1975, Ford and
 113 Diggle 1981, Nance et al. 1988, Valentine et al. 2000). A spatial point process (described below)
 114 is used to simulate \mathbf{n} tree locations, and we use the polygon areas of a Voronoi tessellation based
 115 on point locations generated from a spatial process to define available polygon area (\mathbf{apa}).

116 Available polygon areas are standardized :

$$117 \quad \mathbf{N}_{\mathbf{apa}} = (\mathbf{apa} - \overline{\mathbf{apa}}) / \sqrt{\sum (\mathbf{apa} - \overline{\mathbf{apa}})^2 / (\mathbf{n} - 1)},$$

118 and correlated with vectors of random Normal variables via Wang's (1998) standard Normal
 119 copula algorithm as follows:

120 1) Specify the matrix of partial correlations between available polygon area, diameter and
 121 height:

$$122 \quad \Sigma = \begin{bmatrix} 1 & \rho_{\mathbf{apa},\mathbf{dbh}} & \rho_{\mathbf{apa},\mathbf{ht}} & \rho_{\mathbf{apa},\mathbf{cr}} \\ \rho_{\mathbf{dbh},\mathbf{apa}} & 1 & \rho_{\mathbf{dbh},\mathbf{ht}} & \rho_{\mathbf{dbh},\mathbf{cr}} \\ \rho_{\mathbf{ht},\mathbf{apa}} & \rho_{\mathbf{ht},\mathbf{dbh}} & 1 & \rho_{\mathbf{ht},\mathbf{cr}} \\ \rho_{\mathbf{cr},\mathbf{apa}} & \rho_{\mathbf{cr},\mathbf{dbh}} & \rho_{\mathbf{cr},\mathbf{ht}} & 1 \end{bmatrix}$$

123 2) Obtain the upper diagonal matrix $[\mathbf{A}]$ such that $\Sigma = \mathbf{A}'\mathbf{A}$. We obtain this using
 124 Choleski's decomposition (Andersen et al. 1999) in R.

125 3) Based on the number of points, \mathbf{n} , generated with the spatial point process, generate three
 126 random standard Normal ($\mathbf{N}(0,1)$) vectors ($\mathbf{N}_{\mathbf{dbh}}, \mathbf{N}_{\mathbf{ht}}, \mathbf{N}_{\mathbf{cr}}$) of length \mathbf{n} . The vectors
 127 are column bound with $\mathbf{N}_{\mathbf{apa}}$ to form an augmented matrix, \mathbf{M} :

$$128 \quad \mathbf{M} = [\mathbf{N}_{\mathbf{apa}} \quad \mathbf{N}_{\mathbf{dbh}} \quad \mathbf{N}_{\mathbf{ht}} \quad \mathbf{N}_{\mathbf{cr}}].$$

129 4) The columns of \mathbf{M} are then correlated using \mathbf{A} , the upper diagonal decomposition of Σ :

130
$$\mathbf{Z} = |\mathbf{M}| \cdot |\mathbf{A}|.$$

131 Because of the structure of \mathbf{A} , the first column of \mathbf{M} , corresponding to $\mathbf{N}_{\mathbf{apa}}$, remains
132 unchanged, and $\mathbf{N}_{\mathbf{dbh}}$, $\mathbf{N}_{\mathbf{ht}}$, and $\mathbf{N}_{\mathbf{cr}}$ are correlated both with the underlying spatial
133 pattern and the dbh-height-crown ratio relationships.

134 5) The Normal margins are stripped by applying the inverse cumulative Normal probability
135 distribution:

136
$$\mathbf{U} = \left[\Phi^{-1}(\mathbf{Z}_{\mathbf{apa}}) \quad \Phi^{-1}(\mathbf{Z}_{\mathbf{dbh}}) \quad \Phi^{-1}(\mathbf{Z}_{\mathbf{ht}}) \right].$$

137 \mathbf{U} is a standard Normal copula (Wang 1998).

138 6) The correlated size-spatial data are then obtained by applying the appropriate cumulative
139 margin distribution functions, $\mathbf{F}_i(\mathbf{u}_i)$, to the columns of \mathbf{U} . For \mathbf{apa} , the cumulative
140 function is the inverse of the standardization formula, or simply the original Voronoi
141 polygon areas. The marginal distribution functions for diameter, height and crown ratio
142 are described below.

143 3.1 Spatial Models

144 We utilize two spatial processes: a Lattice Process and a Thomas Process. The lattice
145 process is used to simulate plantation spacing and is implemented in a custom function in R (R
146 Development Core Team 2009), *rlattice*. This function utilizes the *rlinegrid* function (Baddeley
147 and Turner 2008). Angles for the x-oriented lines and y-oriented lines are specified. The **x-**
148 **angle** and **y-angle** must be of opposite sign and between 0 and 90 degrees to insure that lines
149 intersect. The desired **density** (number of trees within the stand) and the **xy-ratio** must also be
150 specified. The stand area, **density** and **xy-ratio** define the spacing of the x and y lines. The **xy-**

151 **ratio** specifies the relative spacing of x lines versus y lines and if not equal to 1 will result in
152 rectangular spacing. The *rlinegrid* function is used to generate a set of x-lines based on **x-angle**
153 and **x-spacing** and a set of y-lines based on **y-angle** and **y-spacing**. The intersections of the two
154 sets of lines define the lattice points. Random variation is added using the *jitter* function, with a
155 **jitter-factor** parameter that defines how much random variation about the lattice intersection
156 exists. Using a **jitter-factor** greater than 0 is the only method to add inhomogeneity into the
157 lattice process. Examples of a lattice process with and without jittering are shown in figures 1A
158 and 1B.

159 The Thomas process simulates clustering, and utilizes the *rThomas* function which
160 implements a realization of a Thomas cluster process (Baddeley and Turner 2008). As with the
161 lattice process, the desired **density** must be specified. **Density** is then used to calculate the
162 **kappa** parameter (intensity of the parent process) for the *rThomas* function based on the stand
163 area and expected number of points per cluster parent (**mu**). The expected number of points per
164 parent (**mu**) and the standard deviation of displacement about parents (**sigma**) determine the
165 number of points and spatial extent of each cluster. By controlling **mu** and **sigma**, the degree of
166 clustering in the spatial process is controlled. Inhomogeneity can be simulated by specifying the
167 name of an R pixel image (object class *im*) for **mu** rather than a numeric value (see the help
168 pages for *rThomas* for examples of creating pixel images). Figures 1C and 1D illustrate a
169 Thomas process with a low level of clustering and an inhomogeneous Thomas process with high
170 density toward the center and decreasing density toward the edges.

171 After the point process is generated, the Voronoi functions provided in the *tripack*
172 package (Gebhardt 2009) are utilized. The *voronoi.mosaic* function is run to generate the
173 Voronoi polygons and the *voronoi.area* function is used to calculate the area of each Voronoi

174 polygon which is used as our estimate of available polygon area (**apa**) for each tree. Boundary
175 points are torused by default so that edge points have bounded Voronoi polygons. The Voronoi
176 object returned by the *voronoi.mosaic* function forms the base of the data frame used to store tree
177 characteristics.

178 **3.2 Species – Size Distributions**

179 Diameter and height distributions are specified using mixture Weibull distributions (Liu
180 et al. 2002, Zhang and Liu 2006), and crown ratio is specified using a mixture four-parameter
181 Beta distribution. A mixture distribution is defined as a frequency distribution made up of two
182 or more component distributions. The distribution of the i^{th} individual component is described
183 by a specific probability density function (pdf), $\mathbf{f}_i(\mathbf{x})$. Then the general pdf, $\mathbf{f}(\mathbf{x})$ for the mixture
184 distribution is expressed as:

$$185 \quad \mathbf{f}(\mathbf{x}) = \sum_{i=1}^k \mathbf{p}_i \mathbf{f}_i(\mathbf{x}) = \mathbf{p}_1 \mathbf{f}_1(\mathbf{x}) + \mathbf{p}_2 \mathbf{f}_2(\mathbf{x}) + \dots + \mathbf{p}_k \mathbf{f}_k(\mathbf{x}),$$

186 where \mathbf{p}_i = the probability of belonging to component i . In this case, \mathbf{p}_i is derived from species
187 composition and $\mathbf{f}_i(\mathbf{x})$ are species-specific distributions.

188 Species composition can be specified in a number of ways including percentiles,
189 quantiles, or actual densities of each species. During the structure simulation process, the
190 specified composition is converted into a frequency distribution (\mathbf{p}_i) and used to randomly
191 assign species to each tree (point).

192 For diameter, the inverse cumulative two-parameter Weibull distribution function is used
193 to obtain values:

$$194 \quad \mathbf{D}_i = \mathbf{b}_i [-\ln(1 - \mathbf{u})]^{(1/\mathbf{c}_i)},$$

195 where \mathbf{D}_i is diameter of the i^{th} species corresponding to cumulative probability \mathbf{u} ; \mathbf{u} is a
 196 cumulative probability obtained from a standard Normal copula; \mathbf{b}_i is a species-specific Weibull
 197 scale parameter; and \mathbf{c}_i is a species-specific Weibull shape parameter. Species-specific two-
 198 parameter Weibull distributions were used for simulating dbh because of the flexibility of the
 199 Weibull distribution, wide application in forestry, and readily available methods for estimating
 200 the parameters (Bailey and Dell 1973, Hyink and Moser 1983, Little 1983, Robinson 2004).

201 A modified three-parameter reverse Weibull distribution (Robinson 2004) was chosen for
 202 the species-specific height distributions. The cumulative three-parameter Weibull distribution is
 203 given by:

$$\mathbf{F}_i(\mathbf{h} \leq \mathbf{H}) = e^{-\left(\frac{\mathbf{a}_i - \mathbf{H}}{\mathbf{b}_i^*}\right)^{\mathbf{c}_i}}$$

204 where, \mathbf{a}_i is a species-specific maximum height ($\max(\mathbf{H}) - \mathbf{H}_B$); \mathbf{b}_i^* is a species-specific scale
 205 parameter; and \mathbf{c}_i is a species-specific shape parameter. The scale parameter, \mathbf{b}_i^* , is defined in
 206 reverse from the maximum, \mathbf{a}_i , and would be interpreted as distance below maximum height.
 207

208 \mathbf{H}_B is the height at which diameter is measured, typically referred to as breast height (1.3 m in
 209 metric and 4.5 ft in Imperial). In order to make the scale parameter interpretable in terms of tree
 210 height, we use $\mathbf{b}_i^* = \mathbf{a}_i - \mathbf{b}_i$. The inverse cumulative distribution function for the modified
 211 reverse Weibull becomes:

$$\mathbf{H}_i = \mathbf{H}_B + \mathbf{a}_i + (\mathbf{b}_i - \mathbf{a}_i)[-\ln(\mathbf{u})]^{(1/\mathbf{c}_i)}.$$

212

213 Inclusion of \mathbf{H}_B insures that no tree is shorter than the height at which diameter is measured.

214 Like the two parameter Weibull distribution, parameter estimation for the three-parameter
215 reverse Weibull is relatively straightforward (Robinson 2004).

216 For crown ratio, \mathbf{CR} , a 4-parameter Beta distribution (Johnson et al. 1995 pp. 210 - 275)
217 is used. The pdf for the four parameter Beta distribution is given by:

$$218 \quad \mathbf{f}(\mathbf{CR}) = \left(\frac{\Gamma(\alpha + \beta)}{\Gamma(\alpha)\Gamma(\beta)} \right) \left(\frac{\mathbf{CR} - \xi}{\lambda - \xi} \right)^{\alpha-1} \left(1 - \frac{\mathbf{CR} - \xi}{\lambda - \xi} \right)^{\beta-1},$$

219 where α and β are the Beta shape parameters, ξ is the minimum crown ratio, λ is the maximum
220 crown ratio, $\Gamma(\bullet)$ is the gamma function, and \mathbf{CR} is the observed crown ratio. Simulated crown
221 ratios are obtained using the *rbeta* function in R using the correlated $U(0,1)$'s from the Normal
222 copula. The *rbeta* function is a two parameter Beta distribution and returns a random variable, \mathbf{Z} ,
223 between 0 and 1. \mathbf{Z} is transformed into crown ratio using:

$$224 \quad \mathbf{CR} = \xi + \mathbf{Z} \cdot (\lambda - \xi).$$

225 The beta parameters are readily estimated using the method of moments or maximum likelihood
226 methods (Johnson et al. 1995 pp. 210 - 275).

227 The mixture distributions are simulated using the following algorithm:

- 228 1) For the \mathbf{n} points generated in the spatial process, species is assigned randomly based on a
229 weighted probability as defined by species composition.
- 230 2) Once species are assigned, then the species-specific distribution parameters are used to
231 calculate diameter, height, and crown ratio using the correlated $U(0,1)$'s from the
232 standard Normal copula as cumulative probabilities .

233 The algorithm is implemented in a custom R function *q.mixed*.

234 **4 THE STAND GENERATOR**

235 The stand generator is developed in the R statistical package (R Development Core Team
236 2009) and is implemented in a custom R function *stand.generate*. We utilize three contributed
237 packages: *spatstat* (Baddeley and Turner 2008); *tripack* (Gebhardt 2009); and *tcltk* (Dalgaard
238 2001). The required inputs, structure generation, and visualization are controlled through a
239 series of input windows built using the tcl/tk interface within R version 2.10.1.

240 The stand generator starts with a main menu window (Figure 2A). The input is divided
241 into three components: Spatial; Species; and Correlation. The Spatial window (Figs. 2B and 2C)
242 allows users to specify spatial information such as dimensions of the stand, desired density, and
243 underlying spatial models. Currently, only rectangular stand areas are supported. Points are
244 torused around the bounding box so that tree locations near the edge will have complete Voronoi
245 polygons. Torusing can be turned off; however, the functions used to calculate the Voronoi
246 polygon areas delete edge points with unbounded Voronoi polygons.

247 Species composition, diameter, height and crown ratio distribution parameters are
248 specified in the Species window (Fig. 2D). Currently the system allows up to 10 species to be
249 specified. The Correlation window (Fig. 2E) allows the user to specify desired correlations
250 between available tree area, diameter, height, and crown ratio.

251 When the Generate button is pressed, the required inputs are used to generate the spatial
252 processes, the voronoi polygon areas, and the trees' species-size distributions. The output is
253 stored in a temporary data frame named *temp.Trees*. Each time Generate is clicked, *temp.Trees* is
254 over written; therefore, if a user wishes to save results, *temp.Trees* must be save to a new file
255 before Generate is relicked. The Visualization window (Fig. 2F) writes an external Stand
256 Visualization System (McGaughey 1997) compatible file and runs SVS (SVS must be installed
257 on the computer) which displays the generated stand structure (Fig. 2G).

258 The R code for the stand generator is available at
259 <http://ifmlab.for.unb.ca/People/Kershaw>. The stand generator will run on all platforms supported
260 by R; however, the visualization step only runs on Windows-based platforms since it utilizes the
261 stand visualization system which is a Windows-based application.

262 **5 EXAMPLES**

263 Data from two different studies are used to demonstrate parameter estimation and test
264 simulation results. The first data set is a 4 ha mapped longleaf pine (*Pinus palustris* Mill.) stand
265 (Platt et al. 1988) consisting of 584 trees. Only diameter at breast height (DBH) and tree
266 locations were measured in this dataset. Total height was predicted using the height – diameter
267 equation found in Shaw and Long (2007). Random error, sampled from a Normal distribution
268 and correlated with available polygon area was added to the predicted heights. Crown ratio was
269 predicted using the crown ratio equation by Acharya (2006) and random error based on the root
270 mean square error was added to the predicted crown ratios from Acharya (2006) so that the
271 resulting predicted crown ratios were correlated with available polygon area. Random errors
272 were added to predicted heights and crown ratios to both add a degree of spatial correlation to
273 the predicted data and reduce correlations within tree parameters. The resulting individual tree
274 summary statistics for this dataset are shown in table 1.

275 The second dataset is a 50 m by 50 m mapped plot located in a mixed species Acadian
276 Forest stand in central New Brunswick. Wooden stakes were surveyed and placed in the ground
277 on a 10 m by 10 m grid. Distance (nearest .01 m) from two adjacent stakes were measured to the
278 face of each tree in each 10m by 10 m block and triangulation, based on side-side-side geometry,
279 was used to determine the xy coordinates of each tree. Tree species was noted, and dbh (nearest
280 0.1 cm) was measured with a diameter tape, and height (nearest 0.1 m) and height to crown base

281 (nearest 0.1 m) were measured with an Optilogic 800LH hypsometer (Opti-Logic Corporation,
282 Tullahoma, TN). There were nine different species in this example: balsam fir (*Abies balsamea*
283 (L.) Mill.); spruce (mostly black spruce (*Picea mariana* (Mill.) Britton, Sterns & Poggenb.) with
284 some red spruce (*Picea mariana* (Mill.) Britton, Sterns & Poggenb.); eastern cedar (*Thuja*
285 *occidentalis* L.); eastern hemlock (*Tsuga canadensis* (L.) Carrière); red maple (*Acer rubrum* L.);
286 white birch (*Betula papyrifera* Marsh.); yellow birch (*Betula alleghaniensis* Britton); white ash
287 (*Fraxinus americana* L.); and American mountain-ash (*Sorbus americana* Marsh.). The
288 individual tree summary statistics by species for this dataset are shown in table 1.

289 **5.1 Parameter Estimation**

290 Thomas spatial processes were used to model spatial locations for both example datasets.
291 Parameters for the Thomas process were estimated using the procedure described by Møller and
292 Waagepetersen (2003 pp. 192 - 197) and Waagepetersen (2008) and implemented in the R
293 function *thomas.estK*. The current version of the stand structure generator only allows a single
294 spatial process for the entire stand; therefore, only a single process was estimated for the mixed
295 species Acadian Forest dataset. The estimated parameters for the Thomas process are shown in
296 table 2.

297 Maximum likelihood estimates of the Weibull shape and scale parameters for the
298 diameter and height distributions were estimated using a modification of Robinson's (2004)
299 algorithm. The minimum measured diameter (2.0 cm dbh for the Longleaf Pine dataset and 8.0
300 cm dbh for the Acadian Forest dataset) were used as the truncation points for the two-parameter
301 left-truncated Weibull distribution (Table 3) and the maximum observed height (plus 0.1 m) for
302 each species was used as the location parameter in the three-parameter reverse Weibull
303 distribution (Table 4). The minimum and maximum crown ratios were used as the bounds of the

304 four parameter Beta distribution. The mean and variance of crown ratio was calculated and
305 moment-based parameter recovery used to estimate the two Beta shape parameters (Table 5).
306 The longleaf pine data were distinctly bimodal in the dbh and height distributions; therefore, the
307 data were divided into overstory trees (trees > 24 cm dbh) and understory trees (trees ≤ 24 cm
308 dbh).

309 The correlation matrix used in the standard Normal copula is the matrix of partial
310 correlations between available polygon area and the tree characteristics. Because the marginal
311 distributions are neither Normal nor the same distribution, we used Spearman's rank correlation
312 coefficient (Zar 1999 pp. 395-398) rather than Pearson's correlation coefficient (Table 6).

313 **5.2 Assessment of Simulated Stand Structures**

314 Fifty simulated stand structures were generated using the estimated parameters from each
315 example dataset. The simulation results were compared to the observed results using the mark
316 correlation coefficient of Stoyan and Stoyan (1994 pp. 262 - 266) as implemented in the R
317 function *markcorr*. Observed and simulated mark correlations versus neighborhood radius are
318 shown in figure 3. While the average mark correlations from the simulated stand structures were
319 smoother than observed correlations, individual simulations often produced local peaks at or near
320 the same spatial scales as the observed data. With the exception of the shorter neighborhood
321 radii, the range of correlations from the simulated data included the observed correlations. This
322 was especially obvious in the Longleaf Pine dataset (Fig. 3A). The smaller range of simulated
323 variability observed in the height (Fig. 3C) and crown ratio (Fig. 3E) in the Longleaf Pine dataset
324 was the result of the high correlations with dbh (Table 6) resulting from the prediction of the
325 these variables using dbh.

326 **6 DISCUSSION AND CONCLUSIONS**

327 The stand structure generator developed in this paper is a simple and efficient method to
328 simulate realistic stand structures. The distributions used to simulate the tree attributes are
329 distributions commonly used in forestry research. The parameters of these distributions are easily
330 estimated from observed data via maximum likelihood methods or moment-based parameter
331 recovery methods. Moment-based parameter recovery methods are especially useful when only
332 stand-level summaries are available (Hyink and Moser 1983). Any distribution could be
333 substituted for those we chose by modifying the input menus and inverse cumulative distribution
334 functions.

335 The use of a Normal copula (Wang 1998) provides an intuitive and fast method for
336 generating the desired spatial dependency. Copulae are applied in many different fields to model
337 complex dependencies (Accioly and Chiyoshi 2004). The critical assumption in the application
338 present in this paper is that available polygon area provides the basic measure of spatial
339 dependency. The available polygon area was proposed by Nance et al. (1988). Here we use
340 Voronoi polygons which are tessellations of the stand area based on perpendicular bisectors of a
341 tree and its immediate neighbors (Bowyer 1981). Nance et al. (1988) proposed weighted
342 polygons, where the division of area was based upon a weighted tree size such that the bisecting
343 line is located further away from the larger tree. This concept is the basis for many distance-
344 dependent measures of competition (Tomé and Burkhart 1989, Stage and Ledermann 2008).
345 While we do not produce weighted polygon areas, the copula produces effects similar such that
346 larger trees tend to be located in larger polygons (assuming the correlation coefficient is
347 positive).

348 A limitation to the copula approach is that all species have the same spatial and intra-tree
349 level correlation coefficients. The system proposed by Valentine et al. (2000) has similar

350 limitations; however, systems based on Gibbs processes can have “repulsive potentials” that vary
351 by species producing spatial patterns that vary by species (Kokkila et al. 2002). The advantage of
352 the copula approach over these other approaches is that trees do not have to be spatially shifted
353 based on potentials (Kokkila et al. 2002, Goreaud et al. 2004) or have tree attributes re-simulated
354 to achieve the desired tree and or spatial distributions (Valentine et al. 2000). Eliminating the
355 need for shifting or re-simulating distributions greatly increases the computational efficiency of
356 our system relative to other systems. Further, the use of the correlation structure to determine the
357 tree attributes (ie, dbh, height, and crown ratio) enables simulation of greater levels of variability
358 and more realistic stand structures than predictive systems that often result in lower variation and
359 greater ordering of tree attributes (ie, largest dbh trees tend to be the tallest, etc.).

360 REFERENCES

- 361 Accioly, R. D. M. E. S., and F. Y. Chiyoshi. 2004. Modeling dependence with copulas: a useful
362 tool for field development decision process. *Journal of Petroleum Science and*
363 *Engineering* 44:83-91.
- 364 Acharya, T. P. 2006. Prediction of Distribution for Total Height and Crown Ratio using Normal
365 versus Other Distributions. Unpubl. M.Sc. Thesis. Auburn University. Retrieved April 6,
366 2010, from <http://etd.auburn.edu/etd/handle/10415/585>.
- 367 Andersen, E., Z. Bai, C. Bischof, S. Blackford, J. Demmel, J. Dongarra, J. Du Croz, A.
368 Greenbaum, S. Hammarling, A. McKenney, and D. Sorensen. 1999. *LAPACK Users'*
369 *Guide, Third Edition*. SIAM, . Retrieved April 5, 2010, from
370 <http://www.netlib.org/lapack/lug/index.html>.
- 371 Baddeley, A., and R. Turner. 2008. spatstat: Spatial Point Pattern analysis, model-fitting,
372 simulation, tests. Retrieved April 5, 2010, from <http://www.spatstat.org/>.

373 Bailey, J. D., and J. C. Tappeiner. 1998. Effects of thinning on structural development in 40- to
374 100-year-old Douglas-fir stands in western Oregon. *Forest Ecology and Management*
375 108:99-113.

376 Bailey, R. L., and T. R. Dell. 1973. Quantifying Diameter Distributions with the Weibull
377 Function. *Forest Science* 19:97-104.

378 Bowyer, A. 1981. Computing Dirichlet tessellations. *The Computer Journal* 24:162-166.

379 Courbaud, B. 1995. Modélisation de la croissance en forêt irrégulière. Perspectives pour les
380 pessières irrégulières de montagne. [Modelling growth in an uneven forest. Anticipating
381 development of irregular *Picea abies* stands in mountain environments.]. *Revue*
382 *Forestière Française* 48:173-182.

383 Dalgaard, P. 2001. The R-Tcl/Tk interface. In: K. Hornik & F. Leisch (eds.), DSC 2001
384 Proceedings of the 2nd International Workshop on Distributed Statistical Computing: 1-9.

385 Eerikäinen, K., J. Miina, and S. Valkonen. 2007. Models for the regeneration establishment and
386 the development of established seedlings in uneven-aged, Norway spruce dominated
387 forest stands of southern Finland. *Forest Ecology and Management* 242:444-461.

388 Ek, A. R., and R. A. Monserud. 1974. FOREST: a computer model for simulating the growth and
389 reproduction of mixed species forest stands. Page 72. Report, School of Natural
390 Resources, College of Agriculture and Life Sciences, University of Wisconsin, Madison,
391 WI.

392 Ford, E. D., and P. J. Diggle. 1981. Competition for Light in a Plant Monoculture Modelled as a
393 Spatial Stochastic Process. *Annals of Botany* 48:481-500.

394 Fox, J. C., H. Bi, and P. K. Ades. 2007a. Spatial dependence and individual-tree growth models:
395 I. Characterising spatial dependence. *Forest Ecology and Management* 245:10-19.

396 Fox, J. C., H. Bi, and P. K. Ades. 2007b. Spatial dependence and individual-tree growth models.
397 II. Modelling spatial dependence. *Forest Ecology and Management* 245:20-30.

398 Garcia, O. 2006. Scale and spatial structure effects on tree size distributions: implications for
399 growth and yield modelling. *Canadian Journal of Forest Research* 36:2983-2993.

400 Gebhardt, A. 2009. tripack: Triangulation of irregularly spaced data. Retrieved April 5, 2010,
401 from <http://cran.r-project.org/index.html>.

402 Genest, C., and J. MacKay. 1986. The Joy of Copulas: Bivariate Distributions with Uniform
403 Marginals. *The American Statistician* 40:280-283.

404 Getzin, S., T. Wiegand, K. Wiegand, and F. He. 2008. Heterogeneity influences spatial patterns
405 and demographics in forest stands. *Journal of Ecology* 96:807-820.

406 Gilliam, F. S. 2007. The Ecological Significance of the Herbaceous Layer in Temperate Forest
407 Ecosystems. *Bioscience* 57:845-858.

408 Goreaud, F., I. Alvarez, B. Courbaud, and F. de Coligny. 2006. Long-Term Influence of the
409 Spatial Structure of an Initial State on the Dynamics of a Forest Growth Model: A
410 Simulation Study Using the Capsis Platform. *Simulation* 82:475-495.

411 Goreaud, F., B. Loussier, M. A. Ngo Bieng, and R. Allain. 2004. Simulating realistic spatial
412 structure for forest stands : a mimetic point process. *Interdisciplinary Spatial Statistics*
413 *Workshop*:22 p.

414 Harrington, T. B., and J. C. Tappeiner. 2007. Silvicultural Guidelines for Creating and Managing
415 Wildlife Habitat in Westside Production Forests. Pages 49-59. General Technical Report,
416 USDA, Forest Service, Pacific Northwest Research Station. Retrieved from
417 http://ifmlab.for.unb.ca/People/Kershaw/PDF_Library/H/HarringtonTB2007b.pdf.

418 Husch, B., T. W. Beers, and J. A. J. Kershaw. 2003. *Forest Mensuration*, 4th edition. Wiley, New

419 York.

420 Hyink, D. M., and J. W. J. Moser. 1983. A Generalized Framework for Projecting Forest Yield
421 and Stand Structure Using Diameter Distributions. *Forest Science* 29:85-95.

422 Johnson, N. L., S. Kotz, and N. Balakrishnan. 1995. *Continuous Univariate Distributions*, 2nd
423 edition. Wiley, New York.

424 Kembel, S. W., and M. R. Dale. 2006. Within-stand spatial structure and relation of boreal
425 canopy and understorey vegetation. *Journal of Vegetation Science* 17:783-790.

426 Kokkila, T., A. Mäkelä, and E. Nikinmaa. 2002. A Method for Generating Stand Structures
427 Using Gibbs Marked Point Process. *Silva Fennica* 36:265-277.

428 Little, S. N. 1983. Weibull diameter distributions for mixed stands of western conifers. *Canadian*
429 *Journal of Forest Research* 13:85-88.

430 Liu, C., L. Zhang, C. J. Davis, D. S. Solomon, and J. H. Gove. 2002. A Finite Mixture Model for
431 Characterizing the Diameter Distributions of Mixed-Species Forest Stands. *Forest*
432 *Science* 48:653-661.

433 Mateu, J., J. Uso', and F. Montes. 1998. The spatial pattern of a forest ecosystem. *Ecological*
434 *Modelling* 108:163-174.

435 McGaughey, R. J. 1997. Visualizing forest stand dynamics using the stand visualization system.
436 1997 ACSM/ASPRS Annual Convention and Exposition 4:248-257.

437 Mitchell, K. J. 1975. Dynamics and Simulated Yield of Douglas-fir. *Forest Science Monographs*
438 17:39.

439 Møller, J., and R. P. Waagepetersen. 2003. *Statistical Inference and Simulation for Spatial Point*
440 *Processes*. Chapman Hall/CRC Press, New York.

441 Nance, W. L., J. E. Grissom, and W. R. Smith. 1988. A new competition index based on

442 weighted and constrained area potentially available. Pages 134-142. General Technical
443 Report, USDA, Forest Service, Ek, A. R., Shifley, S. R., and Burk, T. E. (eds.) Forest
444 growth modeling and prediction. Vol. 1. Proceedings of the August 23-27 IUFRO
445 Conference, Minneapolis, Minnesota. North Central Forest Experiment Station.

446 Nelsen, R. B. 2006. An Introduction to Copulas, 2nd edition. Springer, New York.

447 Oliver, C. D., and B. C. Larson. 1996. Forest Stand Dynamics Updated. Wiley, New York.

448 Pacala, S. W., C. D. Canham, and J. A. J. Silander. 1993. Forest models defined by field
449 measurements: I. The design of a northeastern forest simulator. Canadian Journal of
450 Forest Research 23:1980-1988.

451 Penridge, L. K. 1986. LPOINT: A computer program to simulate a continuum of two-
452 dimensional point patterns from regular, through poisson, to clumped. Page 15. Technical
453 Memorandum, CSIRO Institute of Biological Resources, Division of Water and Land
454 Resources, Canberra.

455 Penttinen, A., D. Stoyan, and H. M. Henttonen. 1992. Marked Point Processes in Forest
456 Statistics. Forest Science 38:806-824.

457 Platt, W. J., G. W. Evans, and S. L. Rathbun. 1988. The Population Dynamics of a Long-Lived
458 Conifer (*Pinus palustris*). The American Naturalist 131:491-525.

459 Pommerening, A. 2006. Evaluating structural indices by reversing forest structural analysis.
460 Forest Ecology and Management 224:266-277.

461 Pommerening, V. A., P. Biber, D. Stoyan, and H. Pretzsch. 2000. Neue Methoden zur Analyse
462 und Charakterisierung von Bestandesstrukturen [New methods for the analysis and
463 characterization of forest stand structures]. Forstwissenschaftliches Centralblatt 119:62-
464 78.

465 Pretzsch, H. 1992. Zur Analyse der räumlichen Bestandesstruktur und der Wuchskonstellation
466 von Einzelbäumen. [Analysis of spatial stand structure and the growth constellation of
467 individual trees.]. *Forst und Holz* 47:408-418.

468 Pretzsch, H. 1997. Analysis and modeling of spatial stand structures. Methodological
469 considerations based on mixed beech-larch stands in Lower Saxony. *Forest Ecology and*
470 *Management* 97:237-253.

471 Pukkala, T. 1988. Effect of spatial distribution of trees on the volume increment of a young Scots
472 pine stand. *Silva Fennica* 22:1-17.

473 R Development Core Team. 2009. R: A Language and Environment for Statistical Computing.
474 Retrieved April 5, 2010, from <http://www.R-project.org>.

475 Robinson, A. 2004. Preserving correlation while modelling diameter distributions. *Canadian*
476 *Journal of Forest Research* 34:221-232.

477 Saunders, M. R., and R. G. Wagner. 2008. Long-term spatial and structural dynamics in Acadian
478 mixedwood stands managed under various silvicultural systems. *Canadian Journal of*
479 *Forest Research* 38:498-517.

480 Shaw, J. D., and J. N. Long. 2007. A Density Management Diagram for Longleaf Pine Stands
481 with Application to Red-Cockaded Woodpecker Habitat. *Southern Journal of Applied*
482 *Forestry* 31:28-38.

483 Smith, K. M., W. S. Keeton, T. M. Donovan, and B. Mitchell. 2008. Stand-Level Forest
484 Structure and Avian Habitat: Scale Dependencies in Predicting Occurrence in a
485 Heterogeneous Forest. *Forest Science* 54:36-46.

486 Stage, A. R., and T. Ledermann. 2008. Effects of competitor spacing in a new class of
487 individual-tree indices of competition: semi-distance-independent indices computed for

488 Bitterlich versus fixed-area plots. *Canadian Journal of Forest Research* 38:890-898.

489 Stoyan, D., and A. Penttinen. 2000. Recent applications of point process methods in forestry
490 statistics. *Statistical Science* 15:61-78.

491 Stoyan, D., and H. Stoyan. 1994. *Fractals, Random Shapes and Point Fields: Methods of*
492 *Geometrical Statistics*. Wiley, New York.

493 Tomé, M., and H. E. Burkhart. 1989. Distance-Dependent Competition Measures for Predicting
494 Growth of Individual Trees. *Forest Science* 35:816-831.

495 Valentine, H. T., D. A. Herman, J. H. Gove, and D. Y. Hollinger. 2000. Initializing a model
496 stand for process-based projection. *Tree Physiology* 20:393-398.

497 Waagepetersen, R. P. 2008. Estimating functions for inhomogeneous spatial point processes with
498 incomplete covariate data. *Biometrika* 95:351-363.

499 Wang, S. S. 1998. Aggregation of Correlated Risk Portfolios: Models & Algorithms.
500 *Proceedings of the Casualty Actuarial Society* 85:848-937.

501 Yamaura, Y., K. Katoh, and T. Takahashi. 2008. Effects of stand, landscape, and spatial
502 variables on bird communities in larch plantations and deciduous forests in central Japan.
503 *Canadian Journal of Forest Research* 38:1223-1243.

504 Yan, J. 2007. Enjoy the Joy of Copulas: With a Package copula. *Journal of Statistical Software*
505 21:1-21.

506 Zar, J. H. 1999. *Biostatistical Analysis*, 4th edition. Prentice Hall, Upper Saddle River, NJ.

507 Zhang, L., and C. Liu. 2006. Fitting irregular diameter distributions of forest stands by Weibull,
508 modified Weibull, and mixture Weibull models. *Journal of Forest Research* 11:369-372.

509

510

511 Table 1. Mean individual tree characteristics by species for the Longleaf Pine and Acadian

512 Forest example datasets. Number of observations appear below species code, and range is shown

513 in parentheses. Height and crown ratio are simulated for the longleaf pine data.

Species ¹	Parameter							
	DBH (cm)		Height (m)		Crown Ratio		Tree Area (m ²)	
	Mean	Std. Dev.	Mean	Std. Dev.	Mean	Std. Dev.	Mean	Std. Dev.
-- Longleaf Pine Dataset --								
LP	26.8	18.33	18.5	9.66	0.53	0.025	68.49	61.446
n=584	(2.0, 75.9)		(1.3, 39.9)		(0.50, 0.73)		(0.52, 407.88)	
-- Acadian Forest Dataset --								
BF	12.4	3.53	11.5	3.39	0.66	0.181	10.59	4.667
n=42	(8.1, 23.3)		(6.4, 18.5)		(0.17, 0.92)		(3.57, 23.01)	
SP	22.7	8.49	17.2	4.63	0.66	0.137	10.43	4.610
n=60	(9.0, 43.9)		(4.7, 24.3)		(0.30, 0.98)		(1.94, 23.66)	
EC	26.1	6.66	15.8	2.88	0.60	0.141	8.14	4.282
n=61	(11.1, 44.4)		(9.3, 21.2)		(0.28, 0.91)		(1.50, 21.16)	
EH	25.4	5.72	13.8	3.40	0.63	0.118	9.52	5.930
n=13	(16.1, 35.3)		(6.8, 17.6)		(0.46, 0.84)		(3.10, 24.25)	
RM	18.5	6.00	17.1	3.29	0.68	0.114	7.69	5.338
n=64	(8.3, 37.2)		(9.1, 24.2)		(0.45, 0.85)		(0.90, 22.33)	
WB	23.7	7.23	19.4	2.85	0.68	0.115	11.75	6.457
n=13	(10.5, 33.1)		(11.9, 23.7)		(0.51, 0.82)		(5.27, 28.41)	
YB	19.8	7.400	16.1	3.95	0.56	0.106	10.02	4.087
n=18	(9.0, 32.9)		(6.4, 22.1)		(0.37, 0.76)		(5.74, 21.02)	
WA	23.9	11.870	18.1	2.98	0.76	0.082	11.17	5.218
n=6	(8.7, 38.0)		(14.0, 23.2)		(0.65, 0.84)		(2.74, 15.52)	
AM	13.7	--	13.7	--	0.71	--	4.15	--
n=1	(--)		(--)		(--)		(--)	

514 ¹LP = longleaf pine; BF = balsam fir; SP = spruce; EC = eastern cedar; EH = eastern hemlock;
515 RM = red maple; WB = white birch; YB = yellow birch; WA = white ash; and AM = American
516 mountain-ash.
517

518 Table 2. Estimated parameters for the Longleaf Pine and Acadian Forest datasets.

Parameter	Dataset	
	Longleaf Pine	Acadian Forest
mu	5.7964	0.3054
sigma	4.1094	0.3204
kappa	2.5188×10^{-3}	0.3378
density (trees in area)	584	258
x-range	{0, 200}	{0, 50}
y-range	{0, 200}	{0, 50}

519

520 Table 3. Maximum likelihood estimates of the two-parameter, left-truncated Weibull distribution
 521 for modelling dbh distributions by species.

Species	Parameter		
	Truncation (min. dbh, cm)	scale (b)	shape (c)
longleaf pine			
understory trees	2.0	8.8774	1.1236
overstory trees	24.0	44.1230	3.5925
balsam fir	8.0	10.1321	2.0094
spruce	8.0	24.9090	2.6850
eastern cedar	8.0	28.6132	4.2684
eastern hemlock	8.0	27.5676	5.3549
red maple	8.0	19.6190	2.8448
white birch	8.0	26.5636	4.3360
yellow birch	8.0	21.1103	2.6357
white ash	8.0	24.5526	1.9063
American mountain-ash ¹	8.0	13.7000	3.6000

522 ¹American mountain-ash had only 1 observation, scale parameter set to the observed dbh and the
 523 shape parameter to be a symmetric distribution.

524

525 Table 4. Maximum likelihood estimates of the three-parameter, reverse Weibull distribution for
 526 modelling height distributions by species.

Species	Parameter		
	location (max. ht., m)	scale ¹ (b)	shape (c)
longleaf pine			
understory trees	22.7	8.3569	2.6615
overstory trees	40.1	25.2362	3.5502
balsam fir	18.6	10.7582	2.0524
spruce	24.4	16.4588	1.5749
eastern cedar	21.3	15.1229	1.9645
eastern hemlock	17.7	13.6660	1.1269
red maple	24.3	16.3058	2.1941
white birch	23.8	19.0692	1.5600
yellow birch	22.2	17.4692	1.4917
white ash	23.3	17.8289	1.3122
American mountain-ash ²	14.7	13.7	3.6

527 ¹scale parameter defined in terms of height above ground, true scale parameter is height below
 528 maximum and is location – scale. ²American mountain-ash only had 1 observation, location was
 529 set 1 m above observed value, scale was set to the observed value, and the shape was set to a
 530 symmetric distribution.

531

532 Table 5. Minimum, maximum, mean and variance of crown ratio by species. Values are used to
 533 obtain parameter recovery estimates of the 4-parameter Beta distribution.

Species	Parameter			
	Minimum	Maximum	Mean	Variance
longleaf pine				
understory trees	0.50	0.56	0.51	0.0001
overstory trees	0.51	0.73	0.54	0.0006
balsam fir	0.16	0.92	0.66	0.03268
spruce	0.30	0.99	0.66	0.01865
eastern cedar	0.27	0.91	0.60	0.01992
eastern hemlock	0.46	0.85	0.63	0.01381
red maple	0.45	0.85	0.67	0.00916
white birch	0.51	0.83	0.68	0.01266
yellow birch	0.36	0.76	0.56	0.01066
white ash	0.65	0.85	0.76	0.00681
American mountain-ash ¹	0.66	0.76	0.71	0.00071

534 ¹American mountain-ash only had 1 observation, minimum and maximum set to .05 below and
 535 above the observed value, and mean and variance set to make a uniform distribution.

536

537 Table 6. Partial correlations, based on Spearman's rank correlation, between available tree area,
538 DBH, height and crown ratio for the Longleaf Pine and Acadian Forest datasets.

Correlation	Dataset	
	Longleaf Pine	Acadian Forest
area – DBH	0.5556	0.1639
area – Height	0.6196	0.1313
area – Crown Ratio	0.7042	-0.1764
DBH – Height	0.9808	0.7118
DBH – Crown Ratio	0.9540	-0.2664
Height – Crown Ratio	0.9849	-0.1564

539

540

541 **Figure Titles**

542 Figure 1. Examples of spatial patterns: A) lattice process with no variation; B) a lattice process
543 with multiplicative jittering; C) a homogeneous Thomas process; and D) an inhomogeneous
544 Thomas process.

545 Figure 2. Input windows for the stand structure generator: A) the main menu; B) the lattice spatial
546 model input window; C) the Thomas spatial model input window; D) the species parameter input
547 window; E) the correlation input window; F) the visualization input window; and G) and
548 example Stand Visualization window.

549 Figure 3. Marked spatial correlations for the example datasets: A) longleaf pine dbh; B) Acadian
550 Forest dbh; C) longleaf pine height; D) Acadian Forest height; E) longleaf pine crown ratio; and
551 F) Acadian Forest crown ratio.

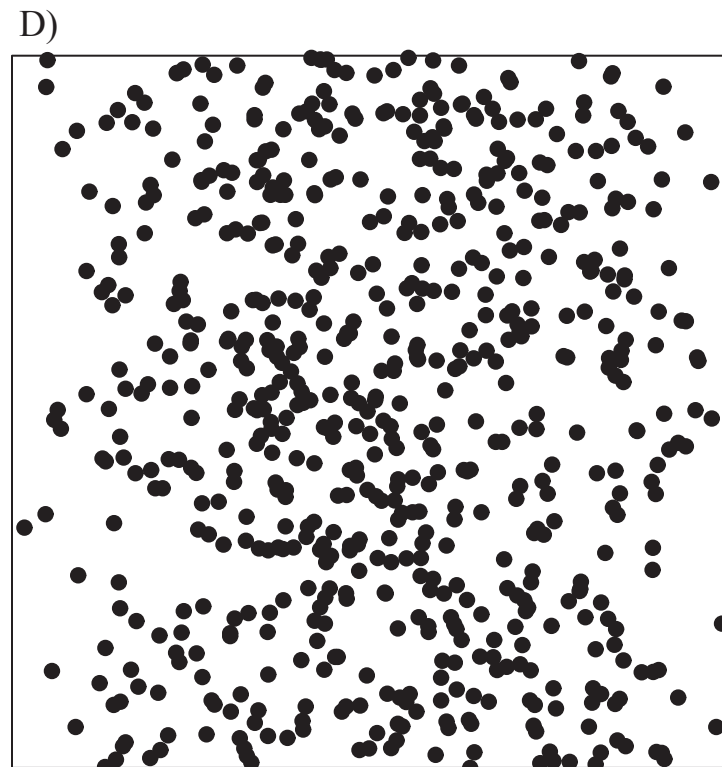
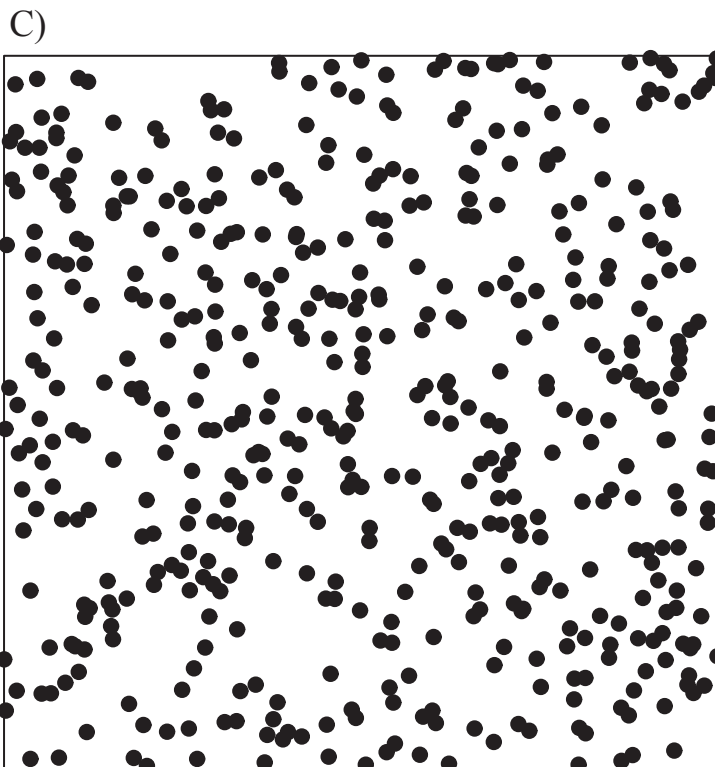
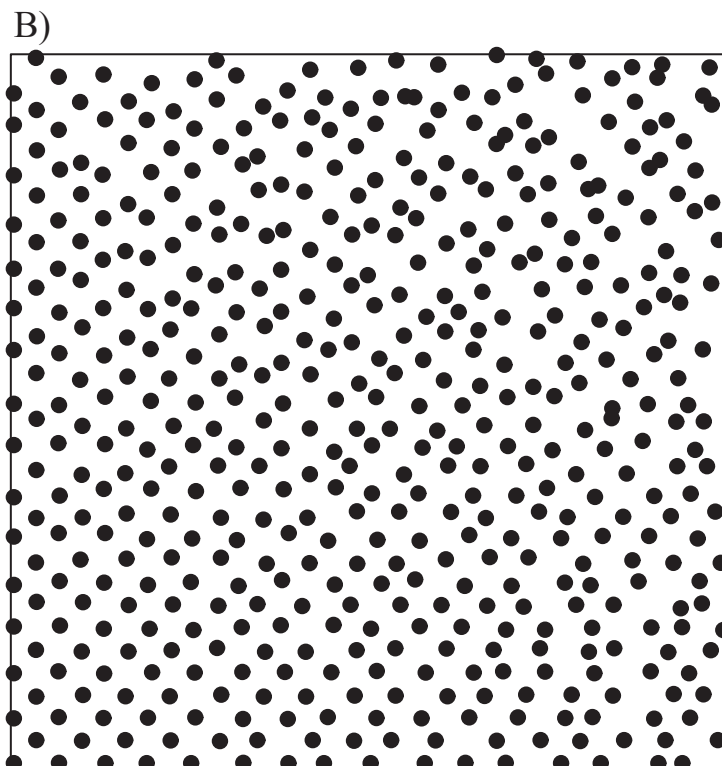
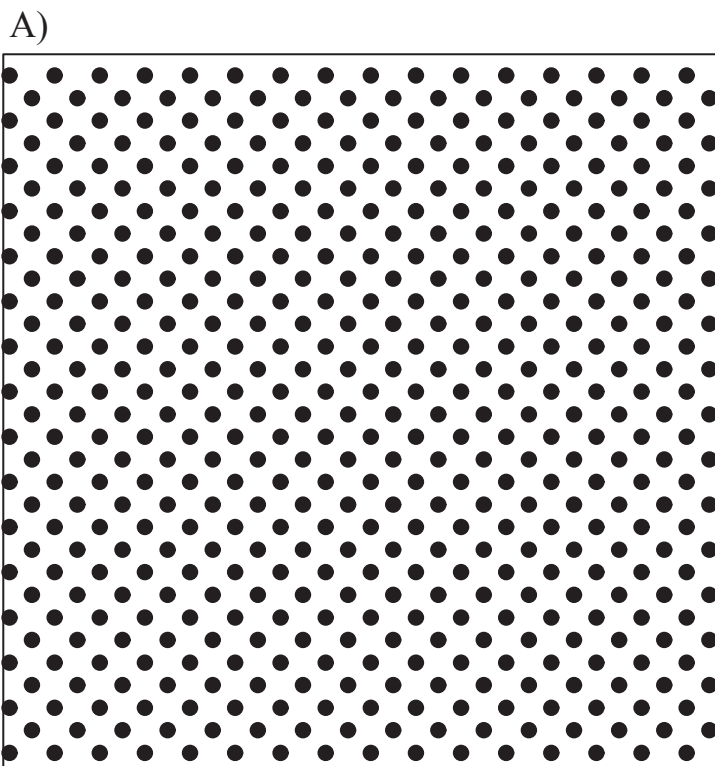


Figure 1

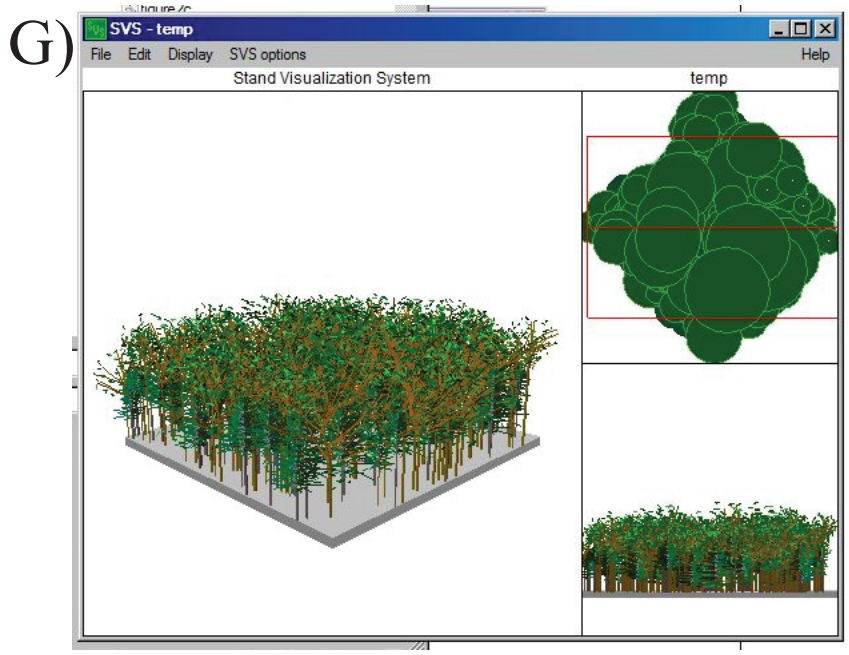
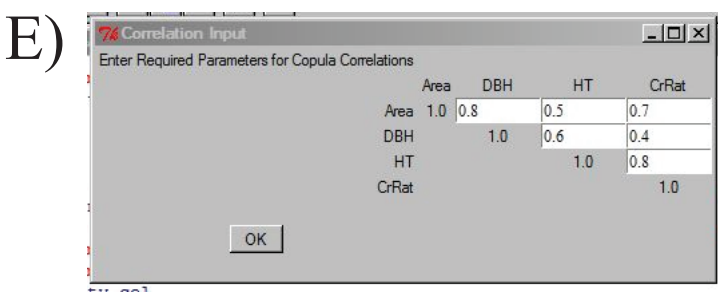
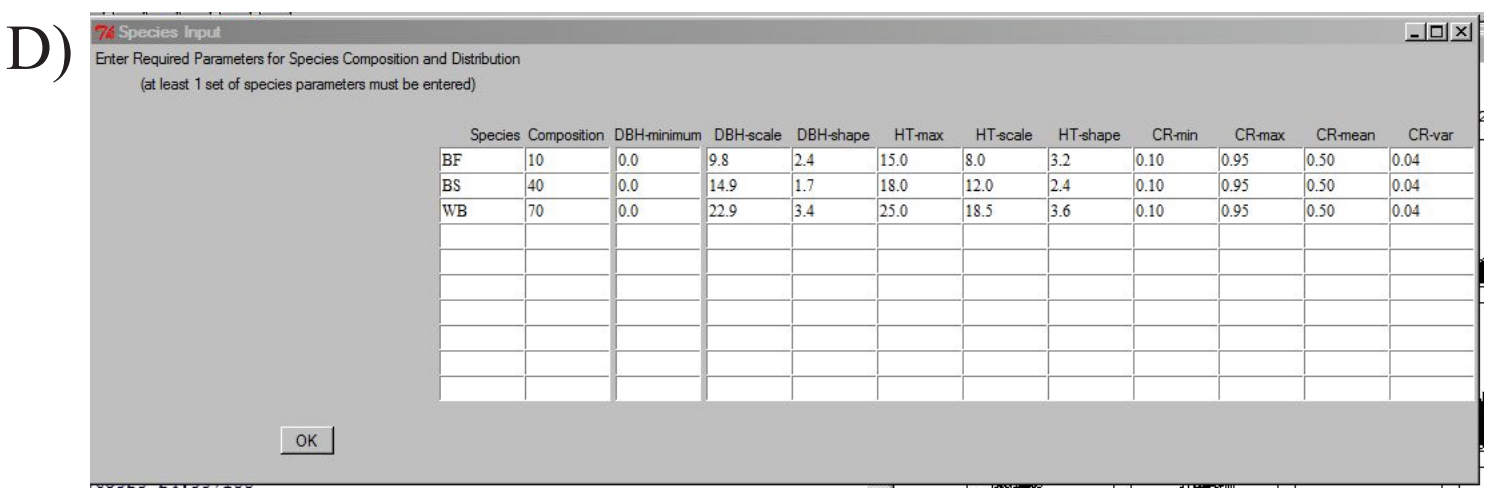
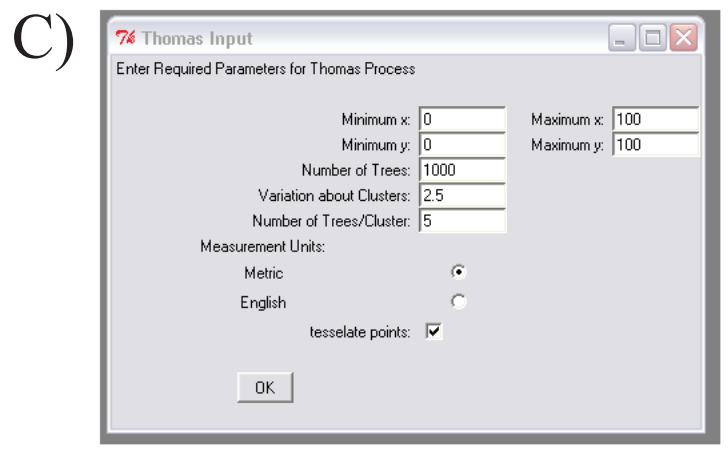
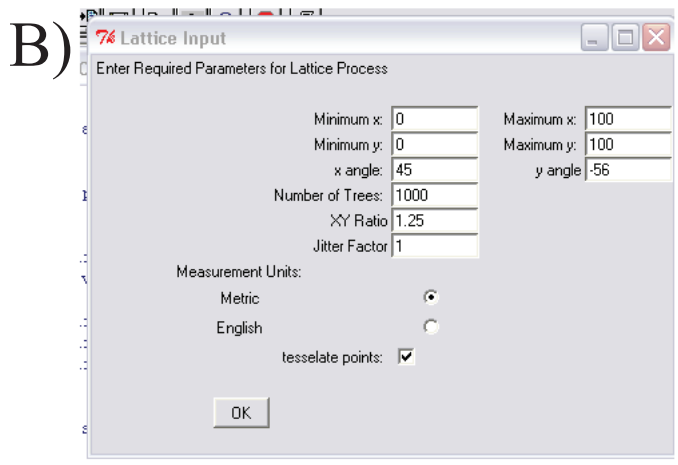
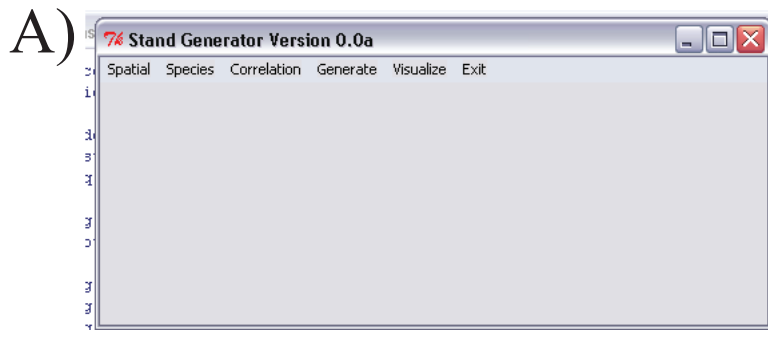


Figure 2

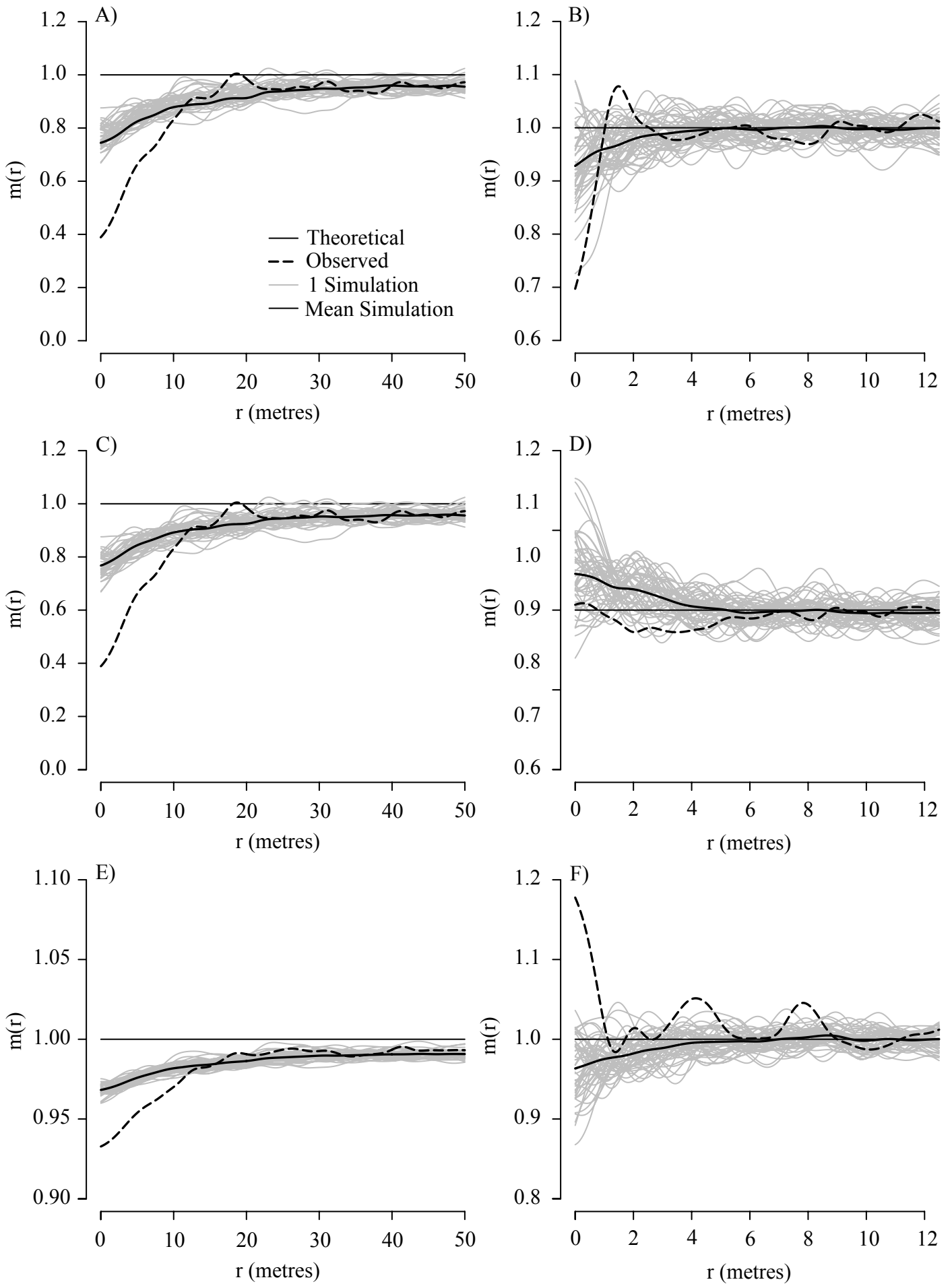


Figure 3